Scale Selective Bias Correction in a Downscaling of Global Analysis using a
Regional Model

Hideki Kanamaru and Masao Kanamitsu

Scripps Institution of Oceanography, University of California, San Diego
La Jolla California

Corresponding author: Hideki Kanamaru, UCSD, Dept. 0224; 9500 Gilman Drive; La Jolla, CA
92093-0224. email: hkanamaru@ucsd.edu

1

ABSTRACT

Systematic large-scale errors are often found within the regional domain in the regional dynamical downscaling procedure. This paper proposes a method to suppress such error using a combination of spectral tendency damping and area average correction of temperature and humidity and surface pressure in the Regional Spectral Model. The scale selective bias correction method reduces the tendency of zonal and meridional wind components for the physical scale greater than a specified scale. In addition, the area mean perturbations of temperature and humidity are forced to zero, and the domain averaged surface pressure perturbation is set to that deduced from temperature and the mean surface elevation between the fine-scale regional model and the coarse base field. Each of these three components of the technique is necessary for the model to reduce large-scale errors in the regional domain effectively. With this method, the regional model is able to generate consistent analyses regardless of domain size. The downscaled field of precipitation compares better with observations, and so do near surface temperature and wind fields. The lateral boundary relaxation is still an essential part of the regional model, but the proposed scheme allows much weaker relaxation. The use of a similar scheme is recommended for any regional model in the application of dynamical downscaling of analysis for climate studies.

1. Introduction

Regional climate models are often used to dynamically produce high-resolution analysis of atmosphere and land that global data assimilation system can resolve only at coarse resolution. When the dynamical downscaling technique is used with reanalyses such as those from the National Centers for Environmental Prediction (NCEP) and the European Centre for Medium-Range Weather Forecasts (ECMWF), all the local details are simulated by the regional model without an input of direct regional-scale observations. What drives the regional model is only the global reanalyses on coarse grids. Therefore, dynamical downscaling can be considered as a "poor person's data assimilation technique" (von Storch 2000) or a "regional data assimilation without regional observation".

Downscaling technique is supposed to retain all the large-scale information that has been resolved well in the global reanalysis data assimilation and to add smaller-scale information that the coarse resolution global data assimilation model could not generate. Regional models, however, have to deal with the problem of lateral boundary conditions, which is mathematically ill posed. The inconsistencies between the model solution and the driving coarse model field along the boundaries produce undesirable noise, and often, instabilities. The lateral boundary relaxation method of Davies (1976) is usually used to alleviate such errors in a buffer zone that covers several grid points along the model boundary.

Systematic large-scale errors could also develop within the regional domain due to model error. Large-scale solutions on the scales that are resolved by the driving global analysis may be trusted and the regional model is not meant to modify such large-scale fields when producing regional solutions. In reality, anomalous long waves that deviate from the

driving coarse large-scale field could be found within the regional domain. Such waves reflect and interfere with shorter waves, distorting the circulation on regional scale. The change in domain averaged temperature and moisture will impact the physical processes through changes in moisture availability and static stability.

Most regional models predict full field within the regional model domain without any knowledge of large-scale features resolved by the driving global analysis except in the buffer zone near the lateral boundaries through Davies-type relaxation. The interior of the domain away from the lateral boundaries does not know the state of large-scale climate in Davies-type relaxation, but the information at the boundary eventually propagates into the domain and provides the large-scale information inside the regional domain.

The notion of using global analysis in the inner domain has led to the "perturbation filter" method first proposed by Hoyer (1987), and used in more practical applications by Juang and Kanamitsu (1994) in the Regional Spectral Model (RSM) originally developed at National Centers for Environmental Prediction (NCEP). Hoyer (1987) and Juang and Kanamitsu (1994) proposed decomposing a full forecast model field within the regional domain into two components: base field and regional perturbation field. The base field is obtained from the global coarse grid over the entire regional model domain. The perturbation is defined as a difference between the total field and the base field, and it is decomposed into sine and cosine series

Most other regional models, however, do not use perturbation method. They predict full regional field in the regional domain. Waldron et al. (1996) suggested a spectral nudging technique that allows incorporation of large internal scales from the outer model into the regional domain for use in "full field" models. A nudging term is added to the tendencies of

4

the variables such as zonal and meridional wind components in their grid point model. The nudging term is the summation of the difference between the spectrally expanded base field and the model field, multiplied by the nudging coefficients over selected wavenumbers. Von Storch et al. (2000) used the technique to nudge the long waves of zonal and meridional wind components in the regional domain to those of the driving fields in a climate simulation study. The nudging term relaxes the selected long wave part of the spectrum to the corresponding waves from the driving fields. Another successful application of spectral nudging is Miguez-Macho et al. (2004)'s exercise in the Regional Atmospheric Modeling System, in which they nudged winds, temperature, and perturbation Exner function.

The RSM calculates perturbation tendencies as a difference between the computed full tendencies and the base field tendencies, and they are transformed to spectral space with a spectral truncation. The spectral truncation filters out those waves longer than the regional domain from the perturbation tendencies. As a result, any scales longer than the regional domain cannot be modified during the course of integration. However, global model and regional model share a common physical scale in their respective spectral ranges (small scale for global but large scale for regional) and long waves within the regional domain are free to develop in RSM. Although the global model field is used in the entire domain, it is only applied to reduce the error due to the Fourier transform of the regional scale field, and there is no explicit forcing towards global model field in the interior of the regional domain. Therefore, RSM is also susceptible to the large-scale error issues that Waldron et al. (1996) and von Storch et al. (2000) addressed.

The basic formulation in RSM is the primitive equation system, consisting of the momentum equation, hydrostatic equation, thermodynamic equation, and mass continuity

equation. The dependent variables are the zonal and meridional component of winds, virtual temperature, specific humidity, and log of surface pressure. The model utilizes a terrain-following sigma coordinate system (28 levels). Model physics are same as NCEP global seasonal forecast model (Kanamitsu et al., 2002) and NCEP/NCAR (National Center for Atmospheric Research) Reanalysis model ((Kalnay et al. 1996), with some differences in convective parameterization and radiation schemes. Therefore, RSM is suitable for climate downscaling with NCEP/NCAR Reanalysis as a forcing.

In this paper, we propose a scheme called Scale Selective Bias Correction (SSBC) which is similar in function to the spectral nudging technique of von Storch et al. (2000) and Miguez-Macho et al. (2004), but this new scheme is developed to work in RSM.

It is noted that the regional dynamical "downscaling" should be clearly distinguished from regional "forecast", since the objectives of the two are very different. The objective of "downscaling" is to obtain regional detail from the large-scale field of reasonably accurate coarse resolution analyses. The objective of "forecast" is to produce good forecast in the regional domain with some reliance, but not entire reliance, on large-scale field produced by global model forecast. In regional "forecast", a regional model may be used to improve the large-scale field in the regional domain, particularly when the regional domain is large, because the large-scale field of global model forecast may contain errors. In regional "downscaling", on the other hand, the regional model should not modify the large-scale field in the regional domain because the large-scale field from the coarse resolution base field is considered accurate. Application of dynamical downscaling to global warming simulation is a little trickier, since global simulation contains significant errors, and regional model may not be able to rely entirely on the lateral forcing. However, it is also difficult to expect

regional model to improve the accuracy of the large-scale portion of the global warming simulations within the regional domain because the one-way nesting prohibits the mutual interactions between global and regional scales. Note that a two-way nesting model cannot be used for "downscaling", since there is no way to force "analysis" or "forecast from other model" through lateral boundary conditions. It is emphasized that this paper specifically discusses the dynamical downscaling of the global analysis, where large-scale analysis is considered to be accurate.

The outline of this paper is as follows. Section 2 discusses experiments. Section 2.1 introduces the Scale Selective Bias Correction (SSBC) method. The function of the method is demonstrated and compared to von Storch's spectral nudging (von Storch et al. 2000) in section 2.2. In section 2.3, we show that our SSBC method works to reduce the dependency of regional solution on the domain size. Each component of the method is also discussed in detail. The choice of damping coefficient and the relation between lateral boundary relaxation and the SSBC method are discussed in section 2.4. Section 3 compares SSBC downscaled fields with observations. Downscaled precipitation field is verified against daily observations (section 3.1). The quality of downscaled climatology surface/near-surface fields is illustrated in section 3.2. Section 4 concludes the paper.

2. Experiments

The Regional Spectral Model (RSM) was originally developed at NCEP and has many model system components in common with the parent model, Global Spectral Model (GSM). In the following experiments, dynamical downscaling of NCEP/NCAR Reanalysis is performed. The model is run over three-month periods in summer (June-August 2000) and in winter (December 2000 – February 2001) for several domain sizes at 60 km grid spacing.

2.1 Scale Selective Bias Correction Method

One of the components of the SSBC is to apply spectral damping to the tendency of variables. By applying implicit time scheme to ensure the numerical stability, the finite difference formulation is shown as:

$$F_t^{new}(m,n) - F_{t-1}(m,n) = \left(\frac{1}{1+\alpha}\right) \cdot \left(F_t^{old}(m,n) - F_{t-1}(m,n)\right) \qquad (1)$$

F_t is a perturbation field spectral coefficient at wavenumbers m and n (in the x and y directions, respectively) at time t in the spectral space. F_{t-1} is the spectral coefficient one time step earlier. The superscripts "*old*" and "*new*" indicate the value before the damping and after the damping, respectively. α is the damping coefficient. In principle, the damping scheme works to reduce the size of the original tendency by multiplying it by coefficient $1/(1+\alpha)$. We choose $\alpha=0.9$ and apply the damping scheme every time step. The choice of $\alpha=0.9$ indicates that the growth of selected long waves are reduced roughly to half. $\alpha=0.9$ worked as well as larger damping coefficient in our experiments (section 2.4) and the results presented in the paper are not sensitive to the choice of damping coefficient.

NCEP/NCAR Reanalysis was run on T62 resolution with its Gaussian grid spacing of roughly 200km. We assume that large-scale features larger than 5-6 grids in size are well resolved in the global Reanalysis model (Pielke, 1991; Laprise, 1992). A set of wavenumbers m and n is chosen such that the damping scheme is applied only to the long waves whose physical wavelengths are 1000km or longer. Note that the use of physical wavelength implies different wavenumber nudging for different domain sizes. This damping is applied only to zonal and meridional wind components uniformly on all sigma levels (UV damping). For the temperature and humidity, we simply set the area mean perturbations to

zero (TQ correction), assuming that the UV damping is strong enough to reduce large-scale errors in the wave component of temperature and moisture. This assumption may need to be refined later, since the dominance of control, i.e., whether winds control mass, or mass controls winds, is dependent on the horizontal and vertical scale of the motion as well as on the latitude. (Kana, this sentence is not very clear) In addition to the large-scale UV damping and TQ correction, the surface pressure perturbation is corrected (surface pressure correction). The difference of mean surface elevation between the regional model and the base coarse grid is calculated. The correct surface pressure perturbation is calculated from the hydrostatic equation with the surface elevation difference and temperature. This is meant to correct the anomalous pressure difference that builds up due to the surface elevation difference (derived from separate orography for global and regional) in the regional model and the global grid. All these corrections together are referred to as the Scale Selective Bias Correction (SSBC) method hereafter. In some sections below, the root mean square difference (RMSD) of pressure height from the base field is used as a measure of regional model error. In these cases, RMSD is calculated for the field for which the scale smaller than 500km is filtered out. This is to assess the impact of the SSBC scheme in reducing the large-scale error in the regional domain by excluding the beneficial RMSD caused by the development of small-scale detail in the domain.

2.2 Reduction of large scale errors

Fig. 1a shows 850-hPa height field difference between the control run (48x35 grids, 2880 km x 2100km domain) of the regional model and the base Reanalysis field, averaged over three months in the winter of 2000-2001. There is a large area-wide positive bias with a

very large positive peak in the west. Such positive bias does not conform to the large-scale solution provided by the base field and could interfere with errors on smaller scales. The area-wide positive bias is eliminated in the SSBC run (Fig. 1b), while the very large positive bias in the western half of the domain is reduced. Fig. 1c illustrates the spectrum of the field as a function of two-dimensional wavenumber. There is a large reduction in wavenumber 1, which corresponds to the removal of area-wide positive bias. Additional few small wavenumbers are also modified for the bias correction of other large-scale features. Medium-sized waves are not influenced by the SSBC but smaller waves (wavenumber 10 or more) are accentuated. Small-scale regional details that were not obvious under the large-scale positive bias become evident in the SSBC run. A few small-scale peaks (Fig.1b) that are as large as 10m in difference from the base field exemplify this function of the scheme. In the same experiment, the winter average 500hPa height field difference from the base field is reduced from an area-wide positive bias of as large as 10m to less than 6m (both positive and negative; not shown).

As described in the previous section, the SSBC method consists of 1) long wave tendency damping on winds (UV damping), 2) TQ correction, and 3) surface pressure correction. It turns out that all these components are necessary to reduce large-scale biases effectively. In order to illustrate the complementary functions of correction components, further experiments were performed. Fig. 2 shows the 500-hPa height difference between the regional model and the Reanalysis field (base field) for the summer of 2000. Fig. 2a is a control run without the SSBC scheme; Fig. 2b uses only the UV damping and TQ correction; Fig. 2c shows the surface pressure correction run only; and Fig. 2d is the simulation with all corrections (full SSBC). The UV damping and TQ correction (Fig. 2b) are able to reduce the

dominant negative peak in the middle of the domain, but most of the area still shows negative bias. The surface pressure correction is able to push up the whole domain by a couple of meters, but the large negative peak is not reduced (Fig. 2c). The scheme is only able to contain the large-scale errors within 6m from the Reanalysis field when all the corrections are combined.

In the large-scale damping part of the SSBC method, winds of the scale greater than 1000km are damped (UV damping), but temperature and humidity are corrected for the area-mean of perturbation only (TQ correction). As opposed to this, von Storch el al. (2000) applied spectral nudging scheme to the zonal and meridional wind components only. The nudging coefficient is applied on the difference between the regional field and the base field (perturbation), as opposed to our scheme that damps the tendency of the perturbation field. RSM was run with von Storch's scheme to see how effective their scheme is compared to the SSBC. Table 1 shows the RMSD of 500-hPa height from the base field for different combinations of spectral nudging and SSBC components. The control run ends up with 11.2m of RMSD and the spectral nudging reduces the error to 8.8m. Our SSBC method can reduce the error to 3.9m, so it is clear that the SSBC is more effective than spectral nudging alone. When only the part of SSBC that damps the longer wave of wind perturbation tendency (UV damping) is applied to the model, the simulation ends up with a comparable RMSD (8.5m) to the spectral nudging alone. In another run, the spectral nudging is complemented with two other components of SSBC (TQ correction and surface pressure correction). The package produces a similar RMSD (4.0m) to SSBC. It appears that the spectral nudging and the UV damping have similar functions.

For regional dynamical downscaling by RSM, TQ correction and surface pressure correction are important players in reducing large-scale errors. The relative importance of UV damping and TQ correction is discussed in the next section. It could be argued that SSBC scheme is not necessary near the surface where the regional model generates its own solutions and so von Storch (2000) chose not to apply his spectral nudging technique below 850 hPa and his nudging coefficient increases with height. We followed this application of spectral nudging to RSM in the experiment above. We apply SSBC scheme, however, regardless of height for the simplicity of the scheme. As seen in Fig. 1c, regional details of near-surface field are not reduced by doing so and the reduction of variance of surface/near-surface fields is small, if any (shown later in section 3.2). Our tests also found downscaling was insensitive to vertical variations of damping coefficient of SSBC.

2.3 Dynamical downscaling and domain size

Dynamically downscaled field should be independent of the domain size, when forced by analysis. We will demonstrate that the SSBC is a powerful method to make the downscaled analysis more independent of the selection of domain, compared to the conventional downscaling without SSBC. Let us suppose that we are interested in downscaling the domain that is half in both x and y directions (24x17 grids, 1440km x 1020km; domain B) from the domain in the previous experiment (48x35 grids, 2880 km x 2100km; domain A). The third domain, C, is approximately 20% larger than domain A in both directions (60x43 grids, 3600km x 2580km) (Fig.3). The three domains are centered in the same point but differ in the expansion. If the model generates very different solutions depending on the domain size, the use of dynamical regional downscaling is limited. Fig.4

shows six panels of 500-hPa height deviation from the base field in the common domain (same as the smallest domain, B) in the winter run. The left column is for control run and the right column is for SSBC-run. Without SSBC, Domains A and C (Fig. 4a and 4c) show similar positive large-scale patterns with 10m maximum in the east, but they are clearly different from domain B, which is more positive over the entire domain on the order of 16m or larger (Fig. 4b). The SSBC method successfully eliminates the biases and the three domains produce strikingly similar patterns (Fig. 4 d-f). The large-scale biases do not exceed 8m with the scheme in any of the domain choices. RMSDs from the base field are calculated for each domain and experiment, as presented in Table 2. Although domain B has the largest errors in the control run, it is reduced by more than 80% in the SSBC run, and the errors in all three domains are less than 3m.

As we discussed in the previous section, UV damping, TQ correction and surface pressure correction are complementary in the SSBC. In light of our interest in making consistent downscaling regardless of domain size, it is necessary to separate UV damping from TQ correction for discussion. In UV damping u and v fields of the scale greater than 1000km are damped, but in TQ correction, temperature and humidity are corrected for the area-mean perturbation only. We made this choice to minimize the use of the damping scheme, yet to obtain the best performance from the scheme. For this short experiment of the first 10-day mean in December 2000, the large domain is 96x69 grid points covering the contiguous United States (5760km x 4140km), and the small domain is 24x17 grid points centered at 100°W and 41°N (1440km x 1020km). As for UV damping, only wavenumber 1 is damped for the small domain, while wavenumbers 1 to 5 are damped in the large domain. TQ correction is in effect, regardless of the domain size. We highlight the difference in the

effect of TQ correction and UV damping over domains with different sizes. The experiments are done for the control (no-SSBC), full SSBC case (with all three components), UV damping and surface pressure correction (no-TQ correction case), and TQ and surface pressure corrections (no-UV damping case).

Figs. 5 show the vertical profile of difference of area-mean temperature from the base field. TQ correction plays a large part, as does the surface pressure correction (Fig. 5a and b). In the control run there are some pressure levels that have an excessively large magnitude of difference from the base field. The top layers of both small and large domain runs, for example, have more than 1 degree difference from the base field area-mean. Such large departures in temperature from the base field are suppressed within 0.2 degrees with the full SSBC run, but the no-TQ correction case still sees those large errors in the top layers. TQ correction is the only component of the scheme that is able to correct such errors. In other levels with moderately sized difference from the base field, both TQ correction and surface pressure correction are effective because the three runs (full SSBC, no-TQ correction, and control) generate markedly different profiles.

One of the reasons why the spectral nudging of von Storch et al. (2000) does not work as well as our SSBC scheme in RSM is that the spectral nudging method changes only the large scale winds as we discussed in section 2.2. It is clear from these area-mean field analyses that TQ correction and surface pressure correction are necessary to nudge the large-scale state of regional downscaled field to the base field in RSM.

It appears that UV damping is not a large player when it comes to the vertical profile of area-mean variables, as indicated by similar profiles between the full SSBC run and the no-UV damping run. Nonetheless, the following experiments show that UV damping is

14

essential in regional downscaling. Figs. 6 show the difference of 500-hPa height from the base field. The left panels are for the small domain and the right panels are for the large domain. In the small domain only the longest wave of u and v winds is damped. The effect of UV damping is minimal because the full SSBC case and no-UV damping case look alike (Fig. 6a and b). The absence of UV damping is compensated by TQ correction. Comparison of the no-TQ correction case (Fig. 6c) with the full SSBC case (Fig. 6a) shows the effect of TQ correction on height field. Thus the UV damping is not effective in the small domain.

In the large domain, the no-UV damping run turns off the damping of the first 1 to 5 wavenumbers of u and v. Its effect should be seen in the large-scale patterns that TQ correction cannot handle. The RMSD is 2.8m in the no-UV damping case, and 2.6m in the full SSBC case. The impact of UV damping is more apparent when looking at Fig. 6d and 6e. The positive peak in the center of the domain and the two negative patterns in the east of the domain are larger in the no-UV damping case (Fig. 6e) compared to the full SSBC case (Fig. 6d). The UV damping reduces the amplitude of waves that those peaks represent in the spectral space, so both positive and negative patterns can be suppressed at the same time.

2.4 Damping coefficient and lateral boundary relaxation

In this section the sensitivity of dynamically downscaled regional fields to the choice of damping coefficient α is tested. The experiments were done at 48x35 grid domain for α of 2, 5, 10, 20, and 100 in winter, and compared with the α=0.9 used in other experiments in this paper. In the largest damping coefficient case, the tendency of perturbation field for selected large waves of winds is reduced to roughly one hundredth of the original, as opposed to one half for the smallest coefficient. The RMSD of 500-hPa height is 6.0m for January in

the control run. January simulations with varying damping coefficients result in a RMSD of

3.3m or smaller, with a decreased RMSD for a larger damping coefficient up to 2.6m for α

=100 (Fig. 7). But a 0.7m reduction in the RMSD by using a large coefficient is not very

significant compared to the large RMSD in the control run. The February control run has a

RMSD of 2.6m, which is already a very small difference, so the SSBC scheme does not have

much impact on the large-scale field. The resulting RMSD for different damping coefficients

are 2.5 to 2.9m. It is not necessarily true that a larger damping coefficient leads to a smaller

RMSD. In December, the RMSD is 12.6m in the control run, which is reduced to 2.5-2.7m

in the SSBC runs, but the largest damping coefficient (α =100) does not yield the smallest

RMSD. It is possible for a different damping coefficient to make small differences in large-

scale field but the difference in RMSD is always less than 1m in 500-hPa height field. The

choice of a larger damping coefficient is not justified by such a small difference. We chose

to use the smallest coefficient as a default.

In order to reduce the noise from the lateral boundaries, RSM uses a lateral boundary

relaxation with implicit time scheme (Juang et al. 1997). One wonders about the relative

importance of the relaxation and the SSBC in the regional dynamical downscaling. Both

share the function of alleviating the inconsistencies between the regional field and base field.

This experiment was done for 96x69 grid domain in summer 2000 with time step of 240 sec.

The relaxation coefficient is 1.0 (the ratio of coarse grid field to the total field) at the

boundary and decreases very sharply to zero away from the boundary towards the inner

domain (see section 3.b of Juang and Kanamitsu 1994 for the formulation and Figure 3 in

Juang and Hong 2001 for the illustration of the function). The width of boundary zone is a

function of grid points in each direction. The boundary zone ends at 12th grid on eastern and

western boundaries and 8th grid on northern and southern boundaries. The default e-folding time for the relaxation is 2400 sec, and the first experiment was done for varying e-folding time between 480 to 3600 sec without SSBC (Fig. 8). The model simulation results in larger RMSD of 500-hPa height from the base field when the relaxation is weaker (larger e-folding time). When the e-folding time is 480 sec, the RMSD is 8.3m and RSME rose to 12.8m when the e-folding time is 3600 sec. Although the relaxation has direct effects only near the boundary by design, it is applied in the grid space and its effect propagates in all spectrums of waves, so large-scale patterns are also affected by the strength of relaxation. The large anomaly in 500-hPa height difference from the base field is over 24m when the relaxation is weak, but it is reduced to about 20m when stronger relaxation is used (not shown). Without the help of SSBC, the easiest strategy to reduce the large-scale error is to decrease the e-folding time and apply a strong boundary relaxation. One needs to be careful, however, of introducing unwanted interaction between regional and global solutions near the boundary due to too strong a relaxation.

The second experiment uses both implicit boundary relaxation and SSBC. The RMSD is about 5m, no matter how weak the boundary relaxation is. The SSBC is much more effective than the strongest boundary relaxation in reducing the 500-hPa height large-scale error. The downscaling runs with the SSBC are able to produce similar simulations, regardless of the strength of boundary relaxation. One is able to use a larger e-folding time and reduce the impact of relaxation, when the relaxation is used with the SSBC. It is not possible, however, to run the model without the relaxation. Our tests show that the model immediately becomes unstable without the relaxation even when the SSBC is turned on. The boundary relaxation is necessary to stabilize the small scale unstable wave excited by the

17

lateral boundary because the SSBC is only applied to large waves and area means. The relaxation is still an essential part of the numerical model even when used together with the SSBC.

3. Comparison with observations

3.1 Daily precipitation field

Large-scale errors in the regional domain could interfere with small-scale dynamics and distort variability in fields such as precipitation. In this section, we assess the performance of the model when SSBC scheme is applied. For the assessment, the model is run for a large domain that covers the entire contiguous United States (96x69 grids), with and without the SSBC scheme. Such a very large model domain ensures a fair skill test of precipitation field against observation. The precipitation observation used for verification is Higgins' gridded daily precipitation for the United States (Higgins et al. 1996). Table 3 shows the equitable threat score (Schaefer 1990) and bias score for the RSM runs in winter and summer. The bias score measures the relative area of simulated and observed precipitation. A perfect score (1) indicates the simulated precipitation area is the same as observed. Bias larger than 1 means overestimated rainfall and bias smaller than 1 means underestimated rainfall. The equitable threat score is the ratio of the correct simulated area to the total area of the simulated and observed precipitation. The score gets penalized for simulating rain in the wrong place as well as not simulating rain in the right place. The higher the value, the better the model skill is for the particular threshold. The scores are computed for the grids that have precipitation above 0.2 mm day^{-1}.

In both seasons threat scores are increased and bias scores are brought closer to 1 in the SSBC runs. In summer, on 60 days out of 92 days threat scores improved by as much as 0.2. Biases are corrected on 55 days. Similarly in winter, threat scores improved on 62 days and bias scores on 71 days out of 90 days. The SSBC demonstrates similarly good skills regardless of season. In other precipitation thresholds of precipitation skill scores for control run ranging from 0.2 to 1.0 mm day^{-1}, summer has dry biases in smaller precipitation range and wet biases in larger precipitation, while winter shows wet biases, regardless of precipitation amount. Both threat scores and bias scores are improved by the SSBC scheme in all precipitation thresholds, but wet biases still remain in large precipitation thresholds.

Fig. 9 shows precipitation fields above 0.2 mm day^{-1} on June 26, 2000. Two downscaled runs (control and SSBC), observation, and NCEP/NCAR Reanalysis are presented. The Reanalysis precipitation would give us a sense of the relationship between the large-scale atmosphere and precipitation distribution. On this day in summer, the threat score improved from 0.42 to 0.53 and the bias score from 0.75 to 0.92 in the SSBC run. The control run (Fig. 9a) has less area of precipitation than the observation (Fig. 9c). In the control run precipitation appears in the southern Great Lakes region, which takes after the spatial pattern of Reanalysis (Fig. 9d) but not the observation. The observation shows precipitation in the Northeast, and over Louisiana, as well as directly to the west of the Great Lakes. Those precipitations are absent in the control run, although they are seen in the Reanalysis. In the SSBC run (Fig. 9b) these deficiencies in the control run have been corrected. The area of precipitation in the southern Great Lakes region breaks up and one part shifts to the west of the Great Lakes while the other moves to the Northeast, although it does not extend as far northeast as the observation. There is more precipitation over

Louisiana as well. The change in the precipitation pattern roughly corresponds to that of the precipitable water pattern (not shown).

Another example of improved precipitation fields is a correction of wet bias on February 11, 2001. The control run (Fig. 10a) shows far too much precipitation in the central United States, compared to the observation (Fig. 10c) and the Reanalysis (Fig. 10d). The precipitable water difference field between the SSBC run and the control run indicates that the control run overestimated precipitable water for most of the country (not shown). The SSBC run eliminated the large precipitable water bias, which led to a marked absence of precipitation in the middle of the continent. The threat score increases from 0.38 to 0.51 and the bias score is reduced from 1.75 to 0.91. In both cases, the correction of large-scale dynamics errors positively influenced the small-scale variability of such fields as precipitable water, and the precipitation field compares better against observation. The SSBC run preserves the correct broad area of precipitation realized in the Reanalysis but fixes the biases and wrong locations are corrected through small-scale dynamics in the regional climate model.

3.2 Climatology of surface/near-surface fields

The SSBC is not supposed to reduce the small spatial scale details that are realized by the regional model when reducing biases in the large scale. We discuss the comparison of daily variance of a couple of downscaled fields between the control run and the SSBC run. Fig. 11 a-b show standard deviation of daily 2m temperature in the summer 2000 (June-August) in control and SSBC run. Larger variance in the north and smaller variance in the south prevail. Fig.11c shows the difference (SSBC minus control) of standard deviation.

Small variance is added over a large extent of the regional domain. There are places with reduced variance but the magnitude is small, if any. The difference in standard deviation is one order smaller than standard deviation itself. Standard deviation of precipitation is much larger than near-surface temperature and reaches more than 10 mm/day in scattered places across the country (Fig. 10d-f). These spots of large variance move locations from the control run to the SSBC, which suggests that the SSBC corrected the location of precipitation and raised the threat score.

Now, we look at the climatology of surface and near-surface fields and compare the SSBC run to the Reanalysis and the North American Regional Reanalysis (NARR, Mesinger et al. 2006). NARR is a data assimilation product by Eta model at 32km grid spacing. Our downscaling runs were performed from T62 NCEP/NCAR Reanalysis to 60km grid spacing and so NARR serves as a good pseudo-observation to check the quality of downscaling. Fig.12a-c show 10m zonal wind of summer 2000 (June-August) in the SSBC run (a), Reanalysis (b), and the NARR (c). The downscaling adds fine scale details to the Reanalysis in correct locations as seen in the agreement between the SSBC run (Fig. 12a) and the NARR (Fig.12c). The global Reanalysis (Fig. 12b) shows too strong wind over Baja California but the downscaled wind (Fig. 12a) agrees well with the NARR (Fig. 12c). The ability of downscaling is particularly evident in 2m temperature field (Fig. 12d-f) when the Reanalysis can only show two broad maxima over the Gulf of California and Texas (Fig. 12e). The SSBC run is able to resolve realistic spatial pattern over the complex topography in the west (Fig. 12d) and the pattern is in good agreement with the NARR (Fig. 12f), although temperature in the Gulf of Mexico is lower in SSBC.

Fig. 13 presents summer precipitation climatology comparison. NARR precipitation field is supposed to be much better than the SSBC run and the global Reanalysis because NARR assimilates precipitation while global Reanalysis does not. As an extra reference, Higgins' precipitation observation is also presented (Fig. 13d). The precipitation amount seems too large especially over the mountains in the west, despite the use of SSBC (Fig. 13a). The bias score from the daily precipitation analysis shows a wet bias for the threshold for larger precipitation amount. Downscaled precipitation's spatial pattern, however, looks very reasonable and precipitation occurs in all the right places, as good threat and bias scores above 0.2 mm/day show (section 3.1). There is no doubt the SSBC worked in favor of better precipitation skill in this regard.

Since large-scale differences in the atmospheric variables are minimized by the use of the SSBC scheme, the remaining large-scale differences in the fields between downscaling and Reanalysis are considered to be caused mainly by the difference in model physics between the RSM and the Reanalysis, namely the convective parameterization and radiation. In general, large-scale components of the fields are very similar between the control and SSBC runs (not shown), but differences are evident in small scale detail, indicating the impact of the SSBC procedure to the small scale that is not directly affected by the scheme.

4. Conclusions

Like any other regional climate model, Regional Spectral Model is not free from the large-scale errors in the regional domain. Despite the use of the global model field not only in the lateral boundary, but also in the inner domain for defining perturbation in the RSM, the model has no explicit forcing towards global model field in the interior of the regional

domain. A correction method to reduce large-scale errors in the RSM dynamical downscaling is formulated. One component of the method is to damp the tendency of selected long wave spectral coefficients of zonal and meridional components of wind, every time step. The cutoff scale of 1000km was used as the smallest accurate scale the global Reanalysis reasonably provides. In addition, domain averaged temperature and humidity perturbations are set to zero. The surface pressure difference between the model field and the global field is also corrected. These corrections are collectively named the Scale Selective Bias Correction (SSBC) scheme.

The SSBC scheme is applied to the downscaling experiments of NCEP/NCAR Reanalysis. The scheme successfully removes large-scale errors in the dynamics field from 500- and 850-hPa height both in summer and winter. The departure of geopotential height from the Reanalysis field of scale greater than 500km does not generally exceed 8m.

Conventional regional climate models could produce an undesirably different picture of downscaled fields depending on the choice of domain size. This shortcoming is proved to be due largely to the large-scale errors that can be reduced by the SSBC scheme. It was demonstrated that the three components of the SSBC scheme are best used together as a package. TQ correction and surface pressure correction are effective no matter how large the domain size. UV damping becomes more important for a larger domain. UV damping is similar in function to the spectral nudging of von Storch et al. (2000), but for RSM the other two functions of SSBC are indispensable.

The optimal coefficient for damping is hard to select without a good measure to determine the skill of the model. Varying coefficients resulted in relatively small differences in 500-hPa height RMSD, so the smallest coefficient was chosen as default. Lateral

boundary relaxation is still a necessary technique for stable model integration, even with SSBC. With the use of the SSBC scheme, one can use a weaker boundary relaxation because SSBC reduces large-scale errors more effectively than relaxation.

It is demonstrated that the SSBC scheme improves the simulation of such fields as precipitation because small-scale dynamics are not disrupted by large scale errors anymore. Experiments are performed over the entire contiguous U.S. and precipitation threat scores increase by about 0.02 in both seasons. The wet bias in winter and dry bias in summer are significantly corrected. Such improvements in the precipitation field resemble patterns of precipitable water change, which responds to the change in the large-scale field. It is not easy to assess the direct benefit of the SSBC scheme on a smaller domain in which precipitation scores are not accurately estimated, but the continental domain experiments proved the scheme's ability to improve the regional scale fields.

Daily variance of small scale structures in the downscaled fields is not sacrificed at the expense of correcting large-scale errors in the regional domain. A comparison of downscaled runs with the North American Regional Analysis proves that the downscaled fine-scale details are real and downscaling added significant values to the global Reanalysis field.

The bias correction method proposed in the paper is not designed only for the Regional Spectral Model. The method is relatively easily applied to conventional grid point regional models, by calculating the difference from the background field over the domain, and applying sine and cosine transforms. It is recommended that when regional models are used for climate simulations such as dynamical downscaling of reanalysis, one must ensure

24

that the large-scale errors are corrected by some method, which would lead to better skill, and consistent downscaled products that are independent of the choice of domain.

REFERENCES

Davies, H. C., 1976: A lateral boundary formulation for multi-level prediction models. *Quart. J. Roy. Meteor. Soc., * **102,** 405-418.

Higgins, R. W., J. E. Janowiak, and Y.-P. Yao, 1996: A gridded hourly precipitation data base for the United States (1963-1993). NCEP/Climate Prediction Center Atlas 1, National Centers for Environmental Prediction, 46pp.

Hoyer, J. M., 1987: The ECMWF spectral limited area model. *ECMWF Workshop Proc. On Techniques for Horizontal Discretization in Numerical Weather Prediction Models,* 343-359.

Juang, H.-M. and S.-Y. Hong. 2001: Sensitivity of the NCEP Regional Spectral Model to Domain Size and Nesting Strategy. *Mon. Wea. Rev.*, **129(12)**, 2904–2922.

Juang, H.-M. H., and M. Kanamitsu, 1994: The NMC Nested Regional Spectral Model, *Mon. Wea. Rev.*, **122**, 3-26.

Juang, H.-M. H., S.-Y. Hong, and M. Kanamitsu, 1997: The NCEP Regional Spectral Model: An Update, *Bull. of Amer. Meteor. Soc.*, **78(10)**, 2125-2143.

Kalnay, E. and Co-authors, 1996: The NCEP/NCAR 40-Year Reanalysis Project. *Bull. of Amer. Meteor. Soc.*, 77, 437-471.

Kanamitsu, M., A. Kumar, H.-M. H. Juang, W. Wang, F. Yang, J. Schemm, S.-Y. Hong, P. Peng, W. Chen and M. Ji, 2002: NCEP Dynamical Seasonal Forecast System 2000. *Bull. Amer. Met. Soc.*, 83, 1019-1037.

Laprise, R., 1992: The resolution of global spectral models. *Bull. Amer. Meteor. Soc.,* **73**, 1453-1454.

Mesinger, F. and Co-authors, 2006: North American Regional Reanalysis. *Bull. of Amer. Meteor. Soc.* **87(3),** 343–360.

Miguez-Macho, G., G. L. Stenchikov, and A. Robock, 2004: Spectral nudging to eliminate the effects of domain position and geometry in regional climate model simulations, *J. of Geophys. Res.*, **109**, D13104, doi:10.1029/2003JD004495.

Pielke, R. A., 1991: A recommended specific definition of "resolution." *Bull. Amer. Meteor. Soc.,* **72**, 1914.

Schaefer, J. T., 1990: The critical success index as an indicator of warning skill. *Wea. Forecasting*, **5**, 570-575.

von Storch, H., H. Langenberg, and F. Feser, 2000: A spectral nudging technique for dynamical downscaling purposes, *Mon. Wea. Rev.*, **128**, 3664-3673.

Waldron, K. M., J. Paegle, and J. D. Horel, 1996: Sensitivity of a spectrally filtered and nudged limited-area model to outer model options, *Mon. Wea. Rev.*, **124**, 529-547.
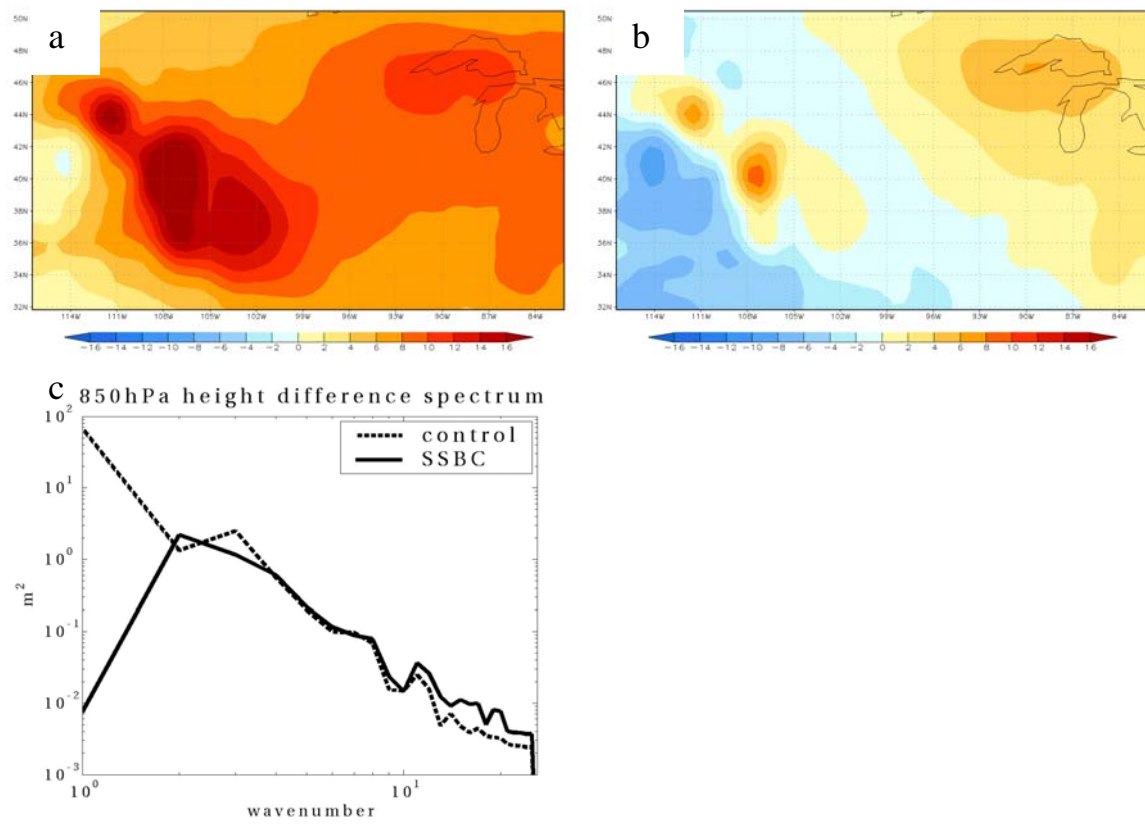
Figure Captions

Fig. 1 850-hPa height difference (m) between the regional model and the Reanalysis in the winter of 2000-2001. a) control run, b) SSBC run, and c) spectrum of both runs.
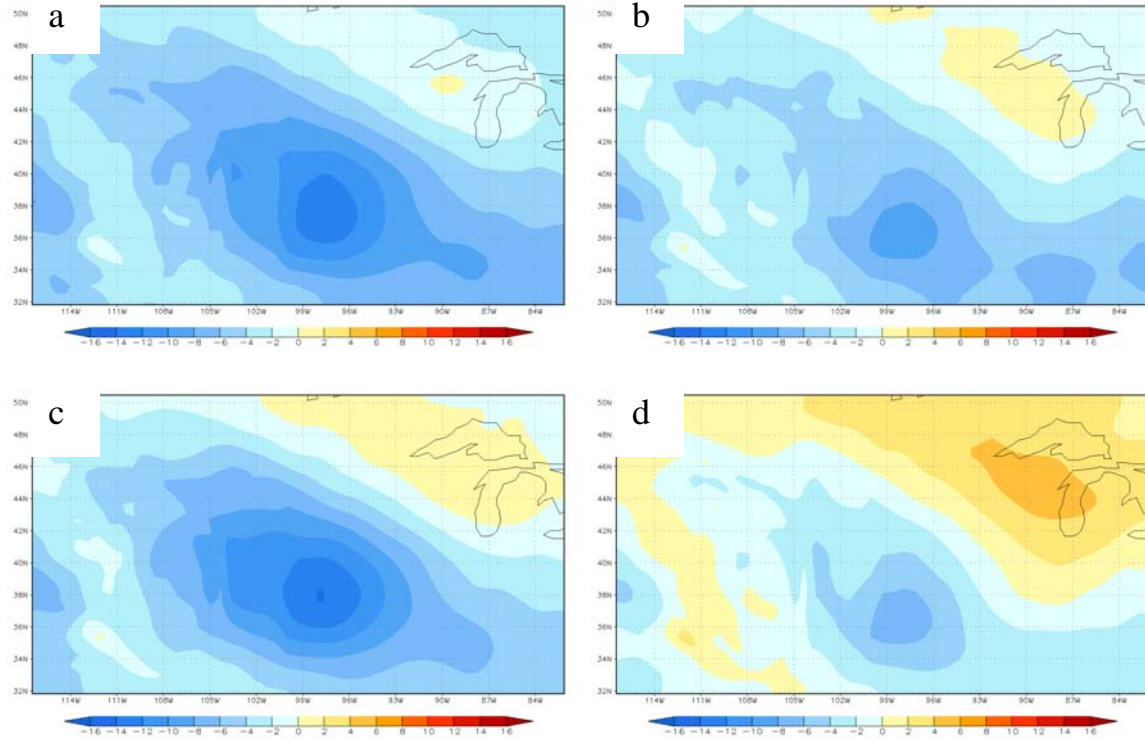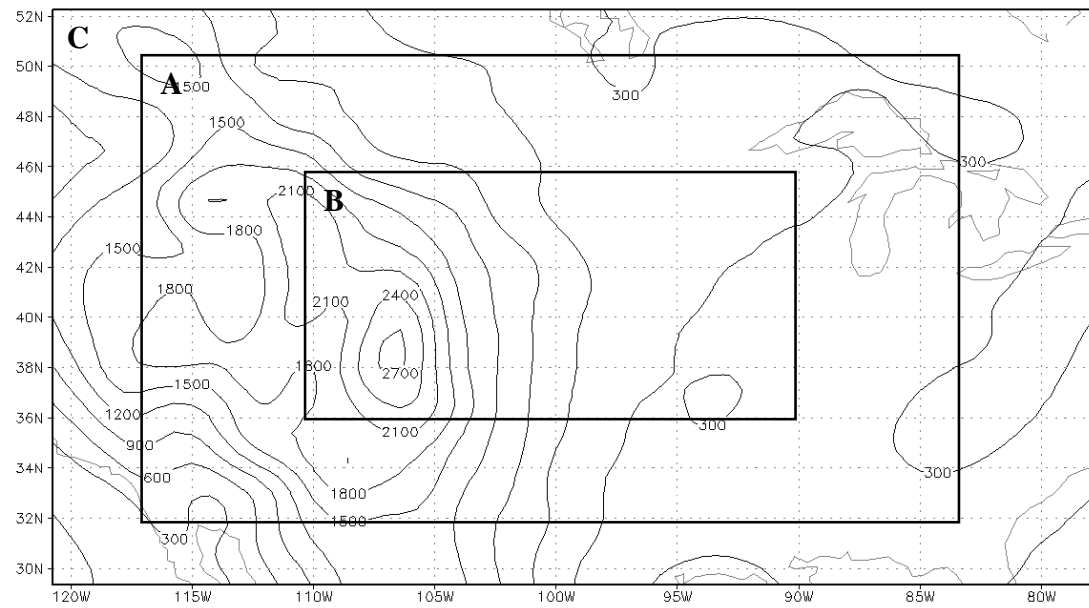
Fig. 2 500-hPa height difference (m) between the regional model and the Reanalysis in the summer of 2000. a) control run, b) long wave damping run (UV damping and TQ correction), c) surface pressure correction run, and d) full SSBC run (both b and c).

Fig.3 Three domain sizes for the experiment. A) 48x35 grids, 2880km x2100km, B) 24x17 grids, 1440kmx1020km, and C) 60x43 grids, 3600km x 2580km.

Fig. 4 500-hPa height difference (m) between the regional model and the Reanalysis, run for different domain sizes and shown for the common area. a) domain A (medium size), control, b) domain B (half of domain A), control, c) domain C (20% larger than domain A), control, d) domain A, SSBC, e) domain B, SSBC, f) domain C, SSBC.

Fig. 5 Area mean difference of temperature (K) from the base field a) small domain b) large domain. Full SSBC and no-UV damping are very similar in both panels.

Fig. 6 500-hPa height difference (m) from the base field. a) full SSBC, small domain, b) no-UV damping, small domain, c) no-TQ correction, small domain, d) full SSBC, large domain, e) no-UV damping, large domain, and f) no-TQ correction, large domain.

Fig.7 Root mean square difference of 500-hPa height from the base field for different damping coefficients.

Fig.8 Root mean square difference of 500-hPa height from the base field for different boundary relaxation e-folding times.

Fig. 9 June 26, 2000 precipitation field above 0.2 mm day^{-1}. a) control run, b) SSBC run, c) observation, and d) global Reanalysis.

Fig. 10 February 11, 2001 precipitation field above 0.2 mm day^{-1}. a) control run, b) SSBC run, c) observation, and d) global Reanalysis.

Fig. 11 Standard deviation of daily 2m temperature (K) in the summer of 2000 (June-August). a) control, b) SSBC, and c) SSBC – control, and daily precipitation (mm day^{-1}) in the summer of 2000 (June-August). d) control, e) SSBC, and f) SSBC – control.

Fig. 12 10m U wind (m sec^{-1}) in summer 2000 (June-August). a) SSBC run, b) global Reanalysis, and c) North American Regional Reanalysis, and 2m temperature (°C) in summer 2000 (June-August). d) SSBC run, e) global Reanalysis, and f) North American Regional Reanalysis.

Fig. 13 Precipitation rate (mm day^{-1}) in summer 2000 (June-August). a) SSBC run, b) global Reanalysis, and c) North American Regional Reanalysis, and d) observation.

Fig. 1 850-hPa height difference (m) between the regional model and the Reanalysis in the winter of 2000-2001. a) control run, b) SSBC run, and c) spectrum of both runs.

Fig. 2 500-hPa height difference (m) between the regional model and the Reanalysis in the summer of 2000. a) control run, b) long wave damping run (UV damping and TQ correction), c) surface pressure correction run, and d) full SSBC run (both b and c).

Fig.3 Three domain sizes for the domain size sensitivity experiment (Fig.4 and Table 2). A) 48x35 grids, 2880km x2100km, B) 24x17 grids, 1440kmx1020km, and C) 60x43 grids, 3600km x 2580km.
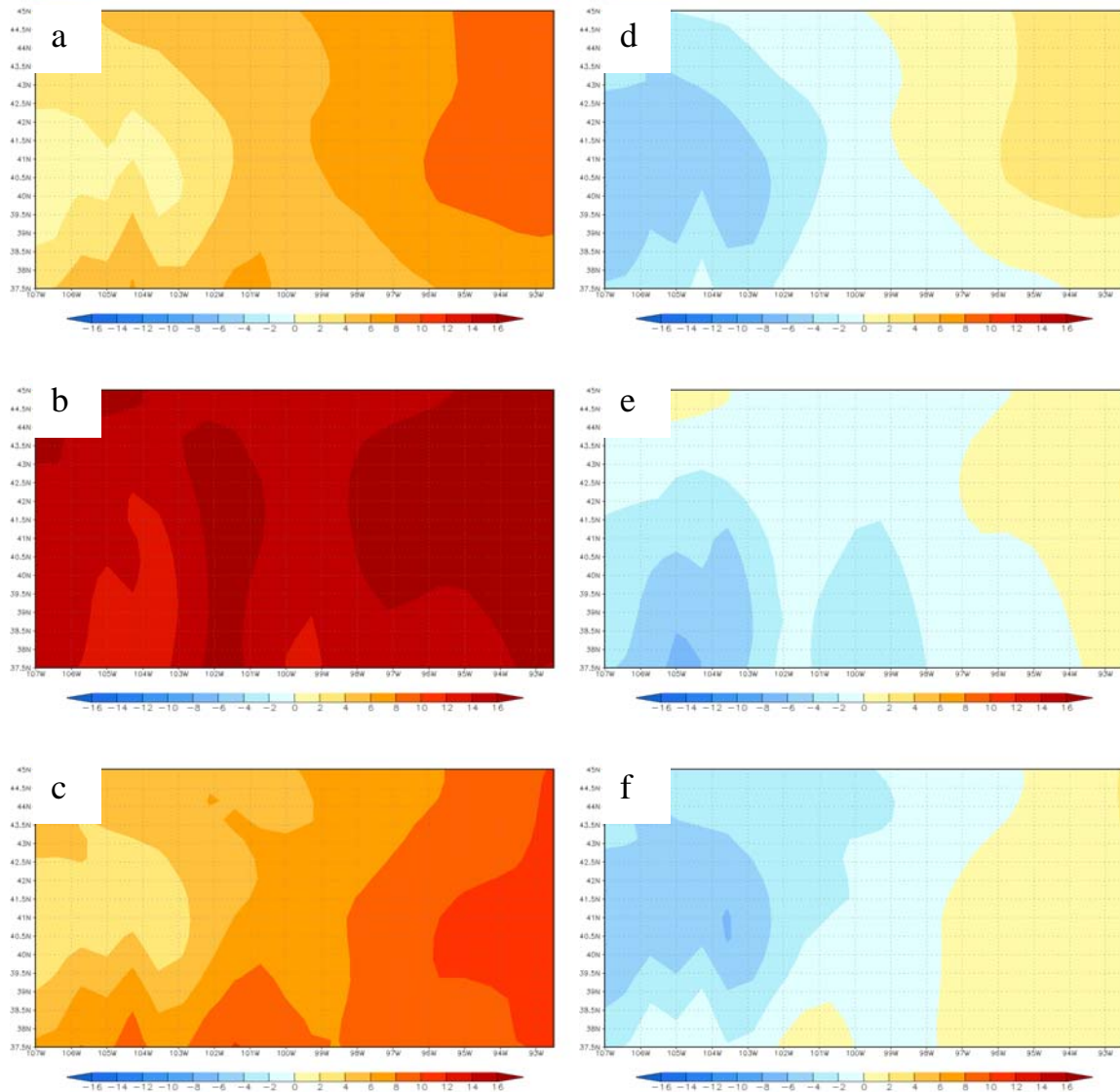
Fig. 4 500-hPa height difference (m) between the regional model and the Reanalysis. The experiment was done for different domain sizes shown in Fig.3. Only the common area (domain B) from each domain is shown for comparison. a) domain A (medium size), control, b) domain B (half of domain A), control, c) domain C (20% larger than domain A), control, d) domain A, SSBC, e) domain B, SSBC, f) domain C, SSBC.
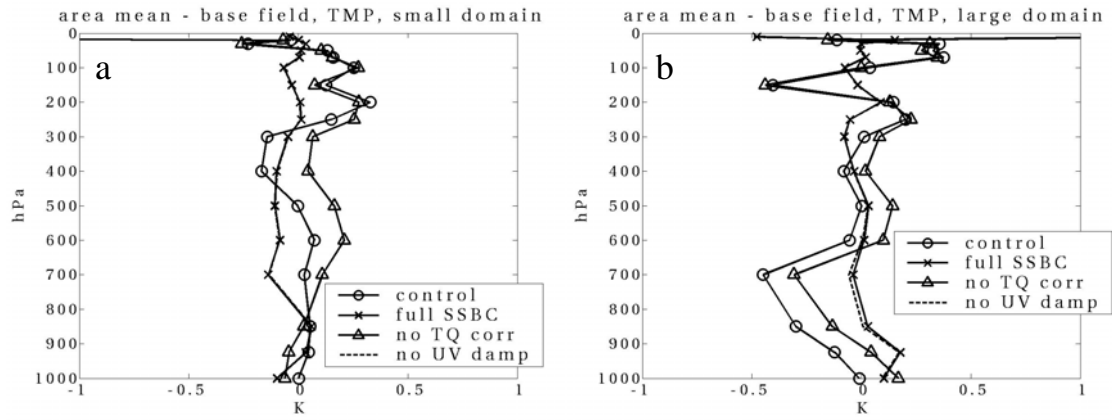
Fig. 5 Vertical profile of area mean difference of temperature (K) from the base field. Each plot shows four cases: control; full SSBC; surface pressure correction and UV damping (no-TQ correction); surface pressure correction and TQ correction (no-UV damping). a) is for small domain (24x17 grids) and b) is for large domain. (96x69 grids). Full SSBC and no-UV damping are very similar and may be hard to distinguish in both panels.
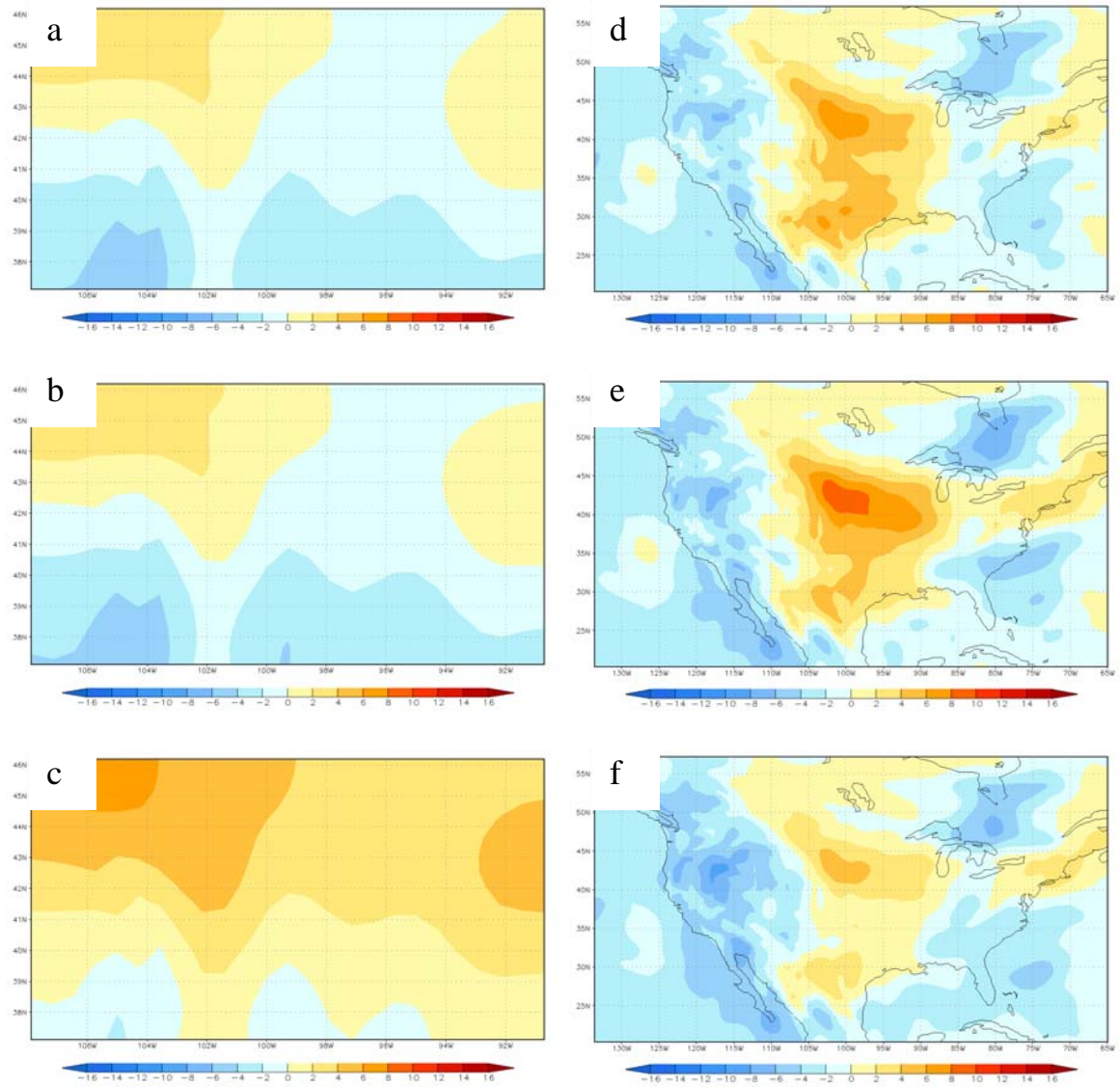
Fig. 6 500-hPa height difference (m) from the base field for the same experiment as Fig. 5. a) full SSBC, small domain, b) no-UV damping, small domain, c) no-TQ correction, small domain, d) full SSBC, large domain, e) no-UV damping, large domain, and f) no-TQ correction, large domain.

35
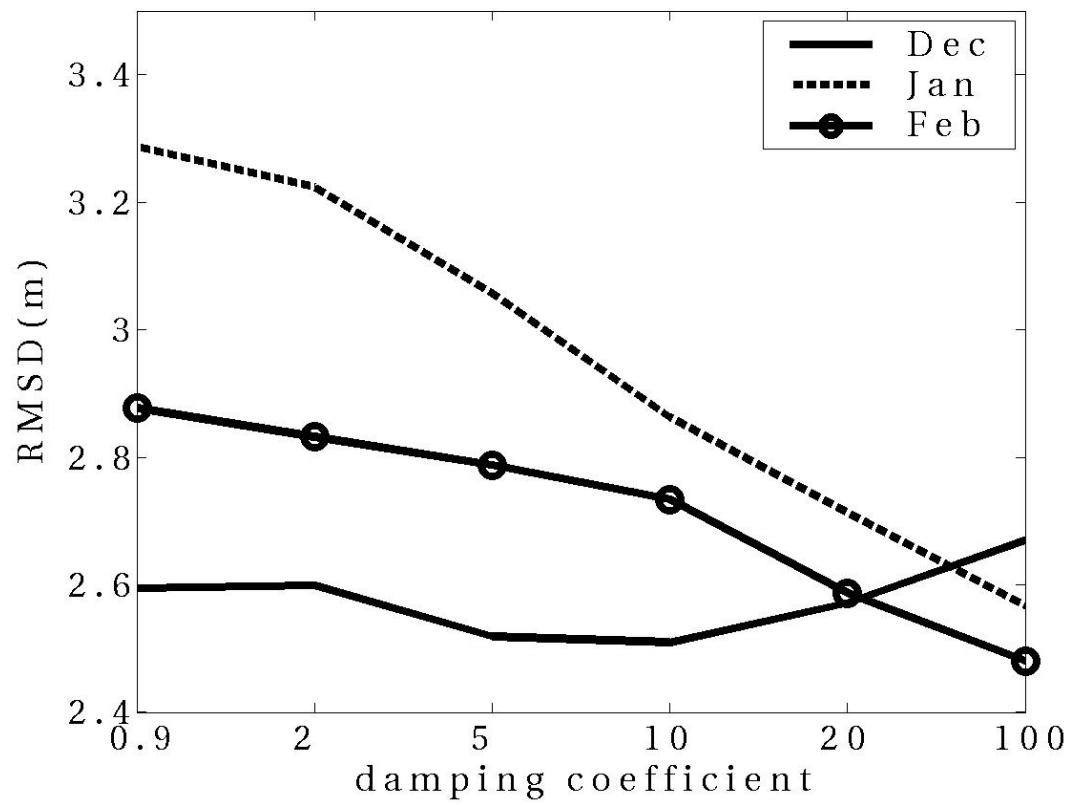
Fig.7 Root mean square difference of 500-hPa height from the base field for different damping coefficients in three winter months.
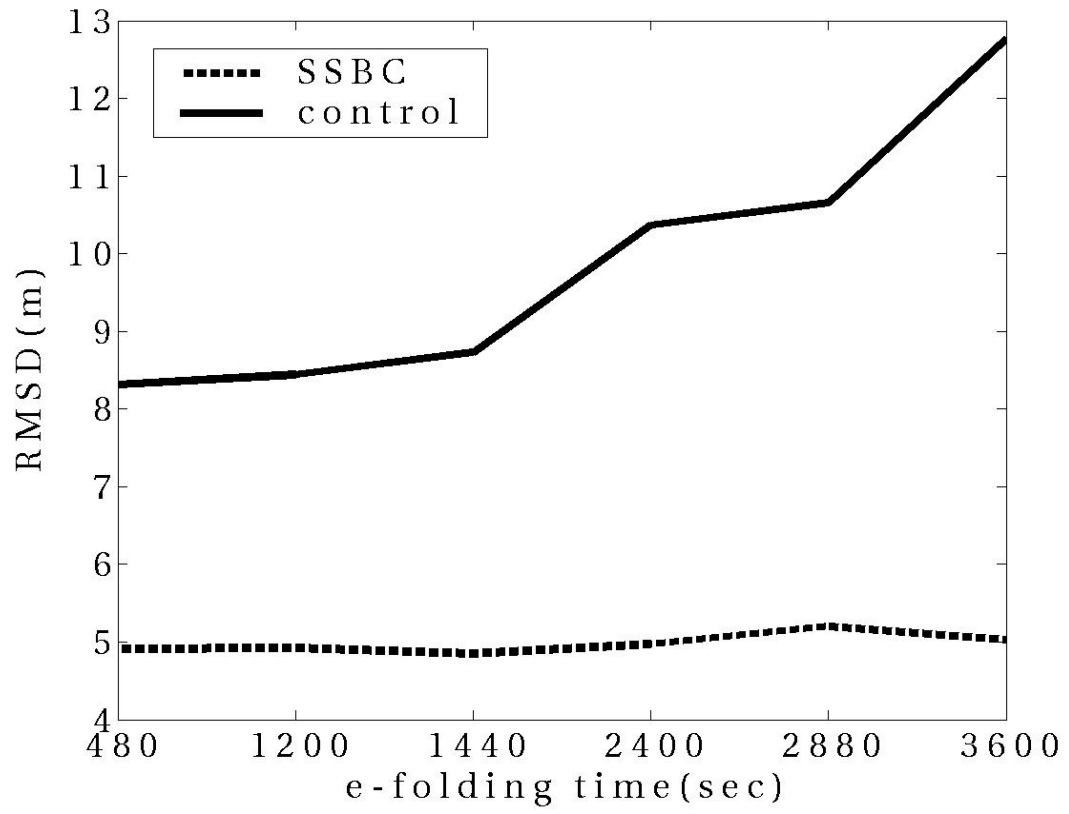
Fig.8 Root mean square difference of 500-hPa height from the base field for different boundary relaxation e-folding times in SSBC and control runs.
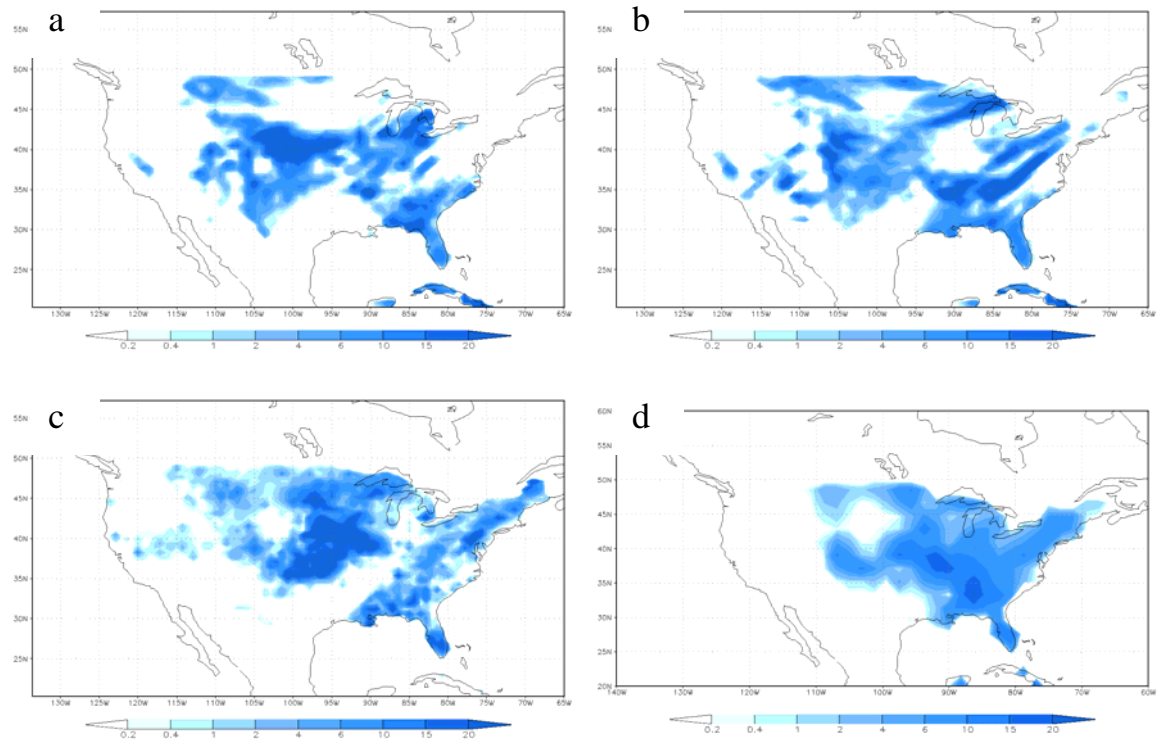
Fig. 9 June 26, 2000 precipitation field above 0.2 mm day^{-1}. a) control run, b) SSBC run, c) Higgins'observation, and d) global Reanalysis.
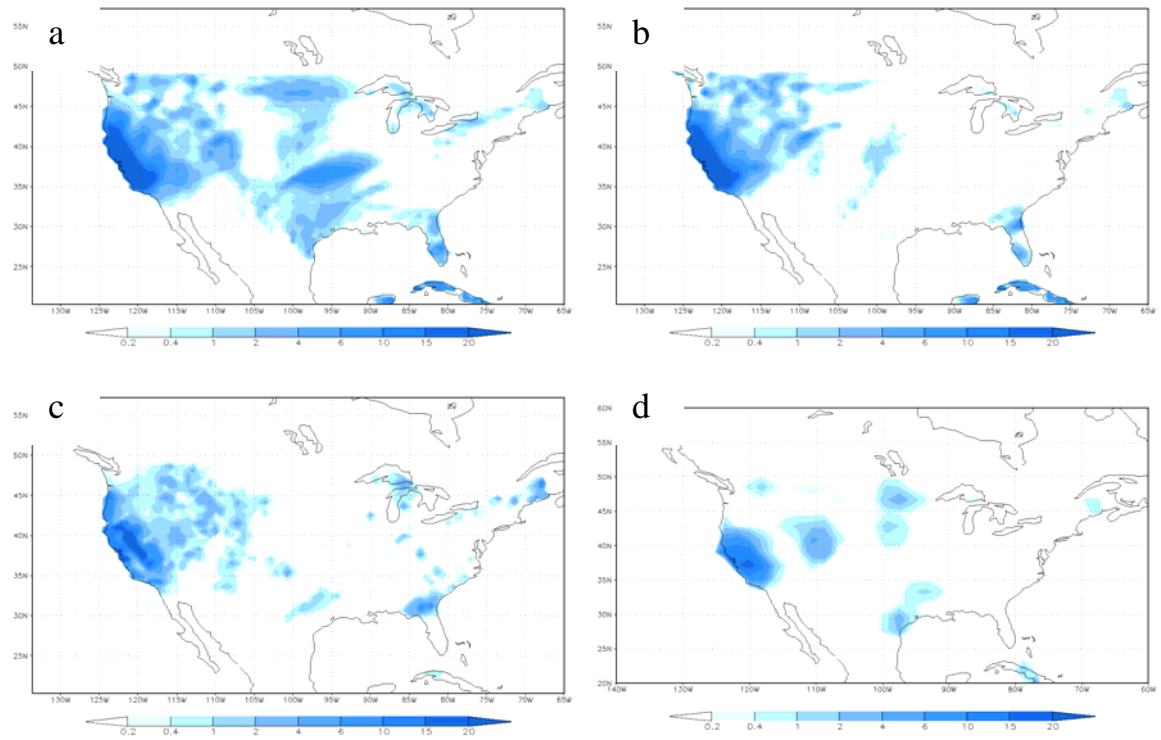
Fig. 10 February 11, 2001 precipitation field above 0.2 mm day^{-1}. a) control run, b) SSBC run, c) Higgins' observation, and d) global Reanalysis.
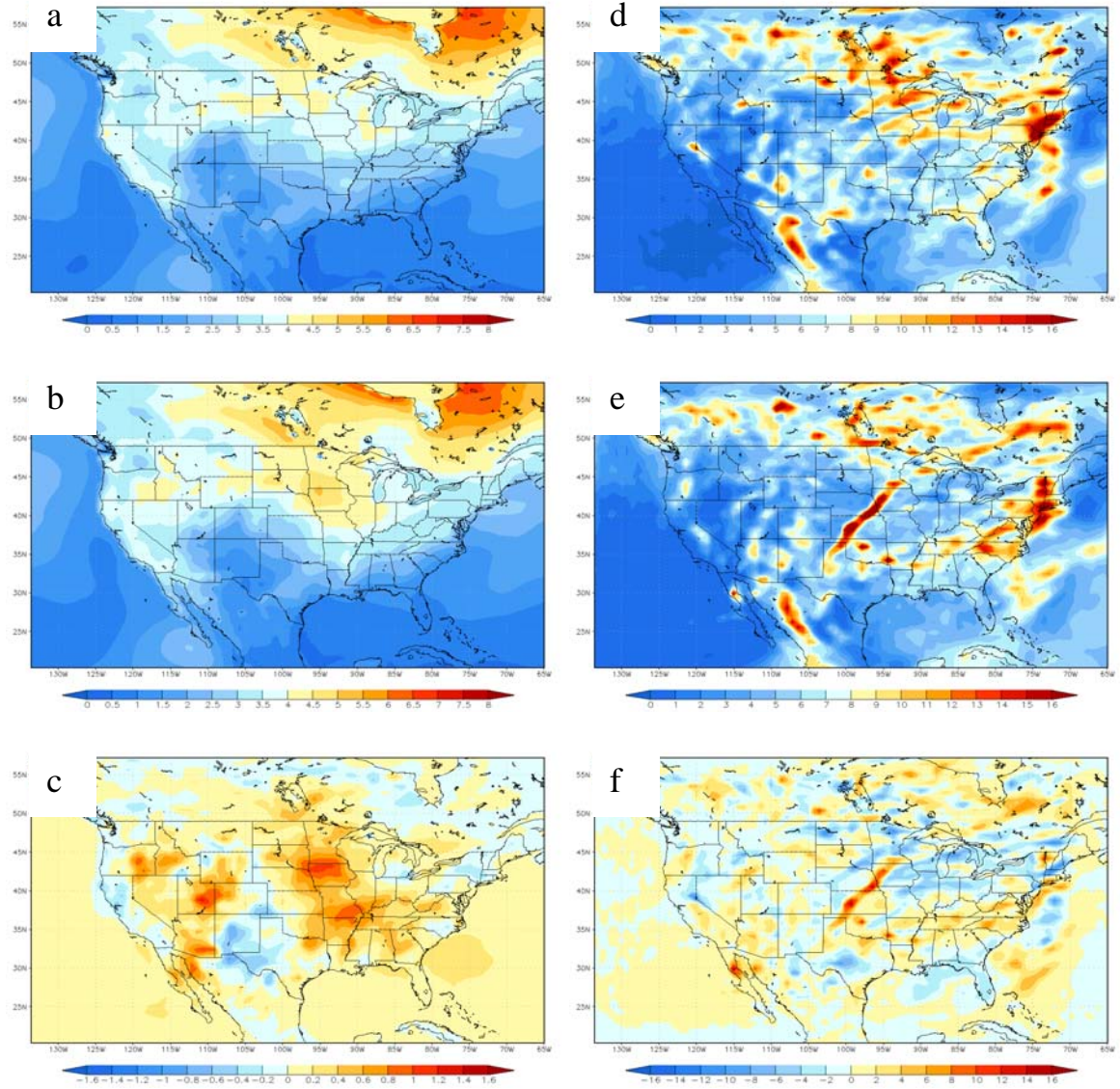
Fig. 11 Left panels are standard deviation of daily 2m temperature (K) in the summer of 2000 (June-August). a) control, b) SSBC, and c) SSBC – control. Right panels are daily precipitation (mm day^{-1}) in the summer of 2000 (June-August). d) control, e) SSBC, and f) SSBC – control.
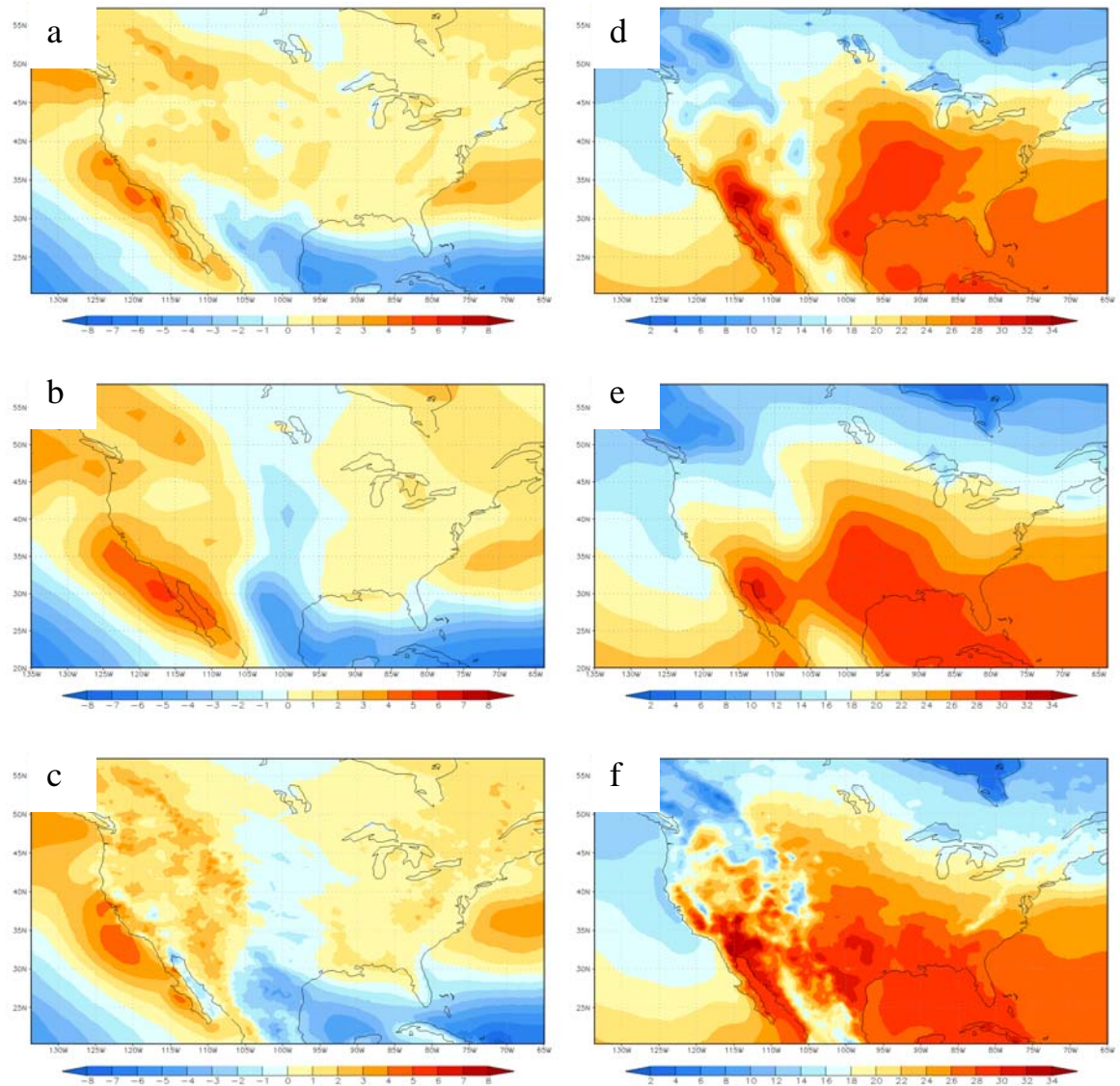
Fig. 12 Left panels are 10m U wind (m sec^{-1}) in summer 2000 (June-August). a) SSBC run, b) global Reanalysis, and c) North American Regional Reanalysis. Right panels are 2m temperature (°C) in summer 2000 (June-August). d) SSBC run, e) global Reanalysis, and f) North American Regional Reanalysis.
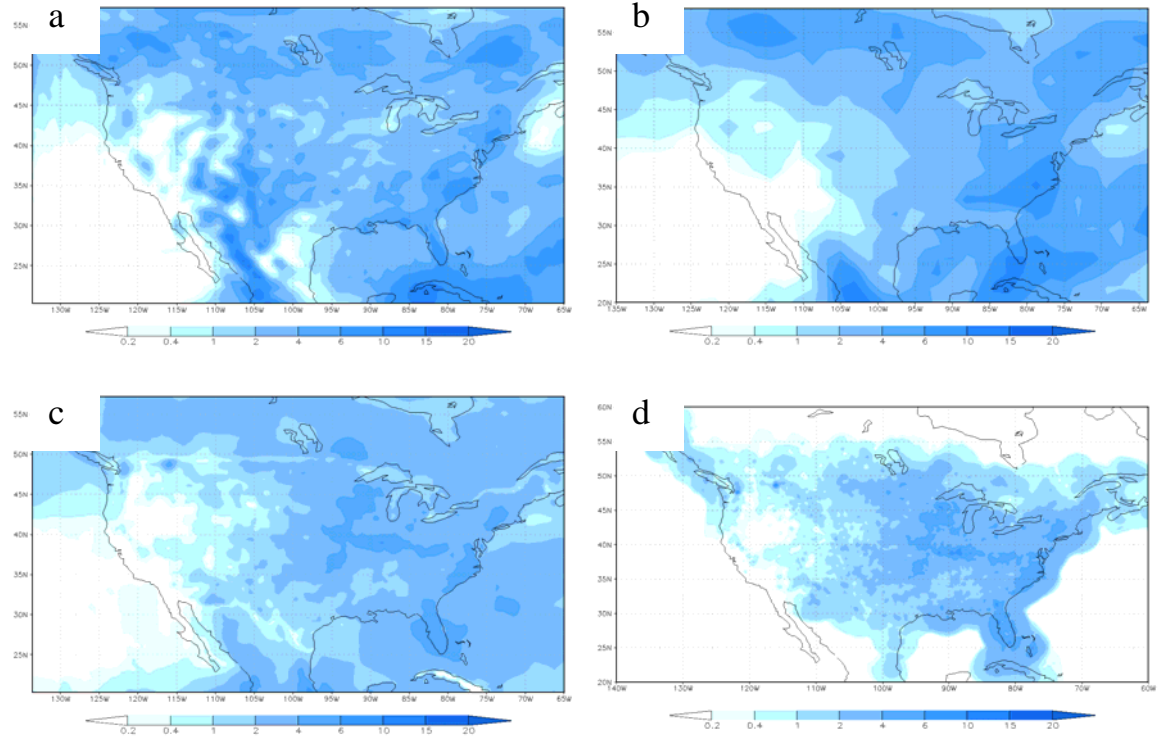
Fig. 13 Precipitation rate (mm day^{-1}) in summer 2000 (June-August). a) SSBC run, b) global Reanalysis, and c) North American Regional Reanalysis, and d) Higgins' observation.

Table 1 Root mean square difference of 500-hPa height from the base field in winter. RMSD is calculated at 500km scale.

	Control	Spectral nudging	UV damping	Spectral nudging + other SSBC functions	SSBC
RMSD (m)	11.2	8.8	8.5	4.0	3.9

Table 2. Root mean square differences of 500-hPa height difference between the regional

model and the Reanalysis field in winter of 2000-2001 calculated for the common area

(domain B) at 500km scale. The model was run on different domains expansion with the

same center point.

	A	B	C
Control	5.9	15.1	7.6
SSBC	2.9	2.4	2.5

Table 3. Precipitation threat scores and bias scores.

	Summer		Winter	
	Threat	Bias	Threat	Bias
Control	0.40	0.95	0.44	1.47
SSBC	0.42	0.97	0.46	1.14